Appl. Phys. B (2014) 117:1135–1140
DOI 10.1007/s00340-014-5936-5

Applied Physics B
Lasers and Optics

Lasing threshold of one- and two-photon-pumped dye-doped silica powder

B. García-Ramiro · M. A. Illarramendi · S. García-Revilla · R. Balda · D. Levy · M. Zayat · J. Fernández

Received: 20 June 2014 / Accepted: 19 September 2014 / Published online: 10 October 2014

Abstract The random laser features around threshold in a ground powder of a silica gel containing Rhodamine 6G-doped silica nanoparticles under one- and two-photon excitation are analyzed. The lasing threshold following two-photon pumping is fifty times higher than after one-photon excitation. Theoretical calculations by using a light diffusive propagation model are in agreement with the experimental results.

1 Introduction

Multiphoton-pumped frequency-upconversion lasing in dye-doped liquid and polymer systems has been one of the most interesting topics in nonlinear optics and quantum electronics in the last years [1]. The main goal pursued was to attain ultrashort wavelength lasing which is useful for data storage, frequency-upconversion imaging, and, not less important, for a better understanding of the interactions between intense optical fields and multiphoton active materials [2]. The principal advantage of lasing upconversion techniques, if compared with other nonlinear processes, is the absence of phase-matching requirements. However, as multiphoton absorption processes are related to high-order nonlinear susceptibilities, high peak power sources are needed to achieve threshold conditions.

On the other hand, linear and nonlinear optical phenomena in fully disordered organic and inorganic systems have received considerable attention due to their important scientific and technological implications. In particular, investigations devoted to light amplification in random structures resulted in the development of a new field of physical optics which gathers various topics such as diffusion, light localization, and nonlinear optics. One of the simplest ways of lasing in random systems is based on gain induced by diffusive feedback provided by disordered-induced light scattering. This feedback mechanism, which is mediated by random fluctuations of the dielectric constant in space, may keep light trapped inside a sample long enough to reach an overall gain higher than losses. To date, laser-like emission has been reported in various scattering material systems from colloidal dye solutions to crystal powders, semiconductor nanoparticles, organic composites, or biological tissues [3–5 and references therein]. In addition, many theoretical analyses and numerical simulations have been constructed in order to study the physics lying behind these radiation sources with a characteristic threshold behavior [6–10]. A detailed discussion of the latest results and theories concerning this phenomenon can be found in Refs. [5, 11–14].

Despite extensively published reports on laser-like emission following one-photon (OP) excitation, just few researchers have addressed the issue of multiphoton-induced random lasing (RL). In 2002, Zacharakis et al. [15]

B. García-Ramiro (✉)
Departamento de Matemática Aplicada, E.U. Ingeniería Técnica Industrial de Bilbao, Paseo Rafael Moreno "Pitxitxi" 3, 48013 Bilbao, Spain
e-mail: mariabegona.garciar@ehu.es

M. A. Illarramendi · S. García-Revilla · R. Balda · J. Fernández
Departamento de Física Aplicada I Escuela Superior de Ingeniería, Universidad del País Vasco UPV/EHU, Alda. Urquijo s/n, 48013 Bilbao, Spain

S. García-Revilla · R. Balda · J. Fernández
Materials Physics Center CSIC-UPV/EHU and Donostia International Physics Center, 20080 San Sebastián, Spain

D. Levy · M. Zayat
CSIC Cantoblanco, Instituto de Ciencia de Materiales de Madrid-ICMM, 28049 Madrid, Spain

firstly observed random laser action using a two-photon (TP) pumping scheme. Such a breakthrough was achieved in dye-doped gelatin cubes pumped with femtosecond laser pulses at 800 nm. Later, Burin et al. [16] investigated within the diffusion model framework, how the nonlinear nature of the excitation modifies the RL threshold, and presented, under several conditions, an analytical result showing a lower lasing threshold for TP pumping than for single-photon excitation. In addition, in 2005, Wang et al. [17] reported a numerical analysis of the saturation effects of the emitted light intensity following TP pumping. It is worthy to notice that the generation of anti-Stokes RL could have a relevant impact due to its applications in the physics of soft matter and biological tissues [18]. In particular, experimental evidences of anti-Stokes random laser emission were found in dye solutions doped with TiO_2 nanoparticles, in micrometer size powder of GaAs, and in ZnO nanoparticles [19–21]. In a preliminary work, the authors experimentally demonstrated TP-pumped RL in a Rhodamine 6G-doped ground powder [22]. The key factor for the occurrence of RL upon high peak power excitation in this material is the high TP absorption cross sections around 800 nm of Rhodamine 6G (Rh6G) if compared to most commercial organic dyes [23 and references therein] together with the efficient scattering feedback of the ground powder. Compared to other dye random media, the advantages of the studied system are its solid-state nature, quenched disorder, high laser-like emission efficiency, and the possibility of being functionalized for various applications such as biomedical sensors.

In this work, we investigate both theoretically (time pulse widths) and experimentally (spectral and temporal pulse widths), the features around threshold of a silica gel powder containing 2 wt%-Rh6G-doped silica (SiO_2) nanoparticles by pumping at one and two photons. The RL is compared under the same sample characteristics (average particle size, volume filling factor) and the same experimental configuration (spot size of the laser). The theoretically predicted pulse shortenings as a function of excitation density, by using a light diffusive propagation model, are in good agreement with the experimental results and reveal that following TP excitation, the random laser threshold of the studied powder is much higher (around fifty times) than with the commonly used OP pumping scheme. A short discussion about the origin of this behavior is given below.

2 Experimental

Silica gel containing 2 wt% Rh6G-SiO_2 nanoparticles was prepared via the sol–gel method. The manufacture details can be found in Ref. [24]. Ground powder of the silica gel with the Rh6G-SiO_2 nanoparticles was obtained by using a mixer mill. Powder polydispersity was evaluated from scanning electron microscope photographs from which an average powder size of around 3 μm was found. The powder sample was compacted in a quartz cell with a larger diameter size (15 mm) and without a front cell window for handling ease and optical characterization. The volume filling factor of the sample ($f = 0.43 \pm 0.05$) was calculated by measuring volume and weight of the samples.

The OP random laser experiments were performed by pumping with the (532 nm) frequency-doubled output of a 20-Hz picosecond Nd:YAG laser (pulse duration of 20 ps). The TP random laser experiments were carried out by using a Ti–sapphire laser system (800 nm) with a pulse duration of 100 fs and a repetition rate of 10 Hz. In both cases, the laser beam was focused to a spot size of 5.6 mm on the sample surface. The resulting emission signal collected in a backscattering geometry was spectrally resolved under both excitation schemes by a fiber-coupled spectrometer and temporally analyzed by a fast photodiode connected to a digital oscilloscope.

3 Experimental results

The general signature of the laser-like emission, that is, the spectral and temporal narrowing of the emission as the pump energy pulse is increased, is illustrated for both types of excitation in Figs. 1 and 2. Normalized emission spectra and temporal profiles obtained below and above random laser threshold under OP and TP excitations have been plotted in Figs. 1a and 2a, respectively. Figure 1b shows the spectral narrowing of the emission by pumping at two schemes, whereas in Fig. 2b we display the experimental temporal narrowing of time profiles. The minimum values of full width at half maximum (FWHM) in Fig. 2b (around 120 ps) correspond to the experimental setup time resolution. The real pulse durations might be narrower. In fact, shorter emission pulses of 50 ps or even less were found in other studies devoted to liquid dyes and polymer sheet random lasers following OP excitation [25–27]. As it can be seen, the spectral and temporal narrowing of the emission under TP pumping takes place at higher pump densities. The point of inflection of a sigmoidal fit through the data points provides the values of random laser threshold. From the fittings shown in Fig. 1b, we obtain the threshold values 0.54 ± 0.01 mJ/cm^2 for OP excitation and 27.2 ± 0.4 mJ/cm^2 for the TP one. The threshold values corresponding to the temporal-narrowing curves plotted in Fig. 2b are 0.54 ± 0.01 and 26 ± 1 mJ/cm^2 for OP excitation and TP excitation, respectively. The sigmoidal fits to the experimental data are represented as dashed lines in Figs. 1b and 2b. The similar threshold values obtained in

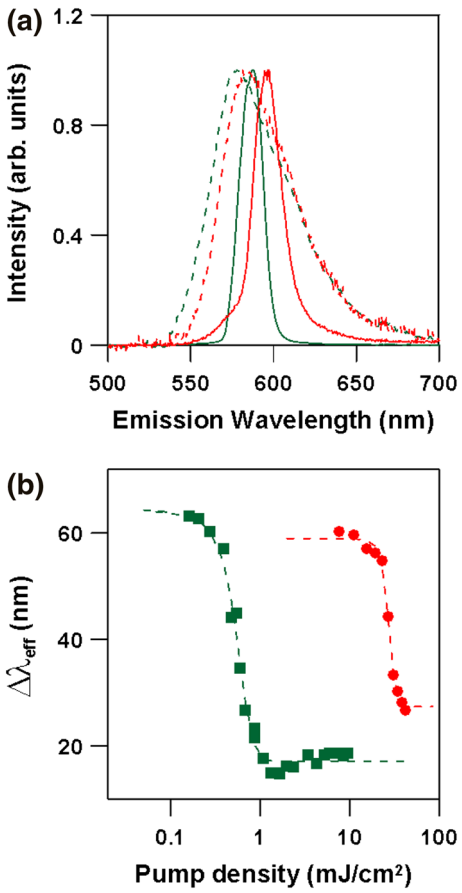

Fig. 1 **a** Normalized emission spectra under OP excitation at 0.2 and 8.4 mJ/cm^2 (*dashed* and *solid green lines*) and TP excitation at 11.5 and 42.2 mJ/cm^2 (*dashed* and *solid red lines*). The *dashed curves* are obtained by pumping below the corresponding random laser threshold, whereas the *solid ones* represent those found above threshold. **b** Spectral narrowing obtained as a function of pump density in the OP (*green squares*) and TP cases (*red dots*). Experimental conditions and powder characteristics are the same in both excitations. The *dashed lines* are the sigmoidal fits to the data

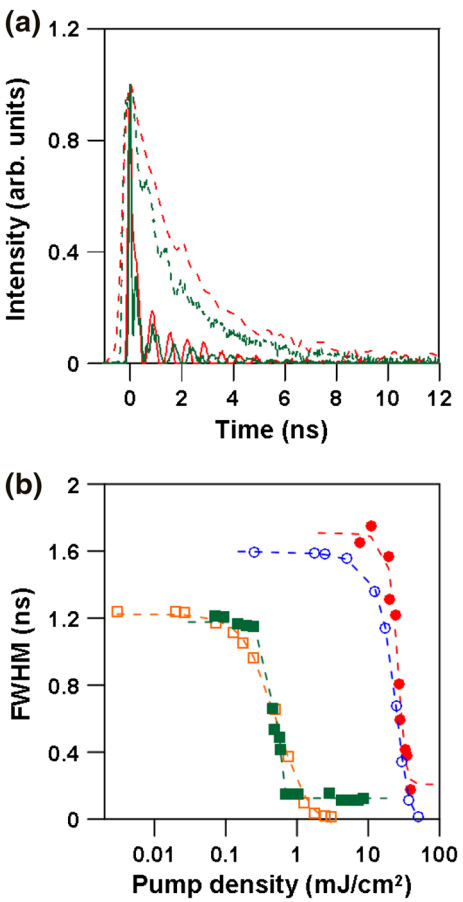

Fig. 2 **a** Normalized temporal profiles obtained under OP excitation at 0.07 and 2.85 mJ/cm^2 (*dashed* and *solid green lines*) and TP excitation at 7.7 and 39.5 mJ/cm^2 (*dashed* and *solid red lines*). The *dashed curves* are obtained by pumping below the corresponding random laser threshold, whereas the *solid ones* represent those found above threshold. **b** Experimental FWHM of the pulses as a function of pump density in the OP (*solid filled green squares*) and TP (*solid filled red circles*) pumping. Theoretical FWHM of the pulses as a function of pump density in the OP (*hollow filled orange squares*) and TP (*hollow filled blue circles*) pumping. Theoretical calculations with: $\lambda_e = 598$ nm, $\sigma_{em} = 2.5 \times 10^{-16}$ cm^2, $n_{eff} = 1.16$, τ_s (OP) = 1.65 ns, τ_s (TP) = 2.1 ns, $f = 0.43$, $K_{abs} = 148.5$ cm^{-1}, and $\beta\,\hbar\,\omega_p = 3.86 \times 10^{-13}$ μm ps. The *dashed lines* are the sigmoidal fits to the data

each pumping condition evidences the parallel behavior in the spectral and time domains.

4 Theoretical model

The light propagation through the ground powders, where the transport mean-free-path is much longer than the light wavelength ($l_t \gg \lambda$), has been described in terms of a diffusion equation [24]. By assuming an incident plane wave along the z-axis upon a slab, whose x and y dimensions are much larger than the z dimension, the generalized time-dependent random laser equations describing our system for both types of excitations are as follows:

$$\frac{\partial W_p(z,t)}{\partial t} = D_p \frac{\partial^2 W_p(z,t)}{\partial z^2} - g(z,t) + p(z,t) \quad (1)$$

$$\frac{\partial W_e(z,t)}{\partial t} = D_e \frac{\partial^2 W_e(z,t)}{\partial z^2} + f\,v\,\sigma_{em} N(z,t) W_e(z,t) + \gamma \frac{N(z,t)}{\tau_s} \quad (2)$$

$$\frac{\partial N(z,t)}{\partial t} = g(z,t) - f\,v\,\sigma_{em} N(z,t) W_e(z,t) - \frac{N(z,t)}{\tau_s} \quad (3)$$

where $W_p(z,t)$ is the light density at the pump wavelengths ($\lambda_p = 532$ nm for OP excitation and $\lambda_p = 800$ nm for TP one), $W_e(z,t)$ is the light density at the emission wavelength ($\lambda_e = 598$ nm), and $N(z,t)$ is the density of dye molecules in the excited state. The term corresponding to light absorption, $g(z,t)$, is given by $g_{OP}(z,t) = f\,v\,K_{abs} W_p(z,t)$ and by $g_{TP}(z,t) = f\,v^2 \beta\,\hbar\,\omega_p W_p^2(z,t)$, for

OP and TP excitations, respectively. K_{abs} is the OP absorption coefficient of the material at the pump wavelength, and β is the TP one. The volume fraction, f, occupied by the scatters has been included in the equations to take into account the effective part of light density which penetrates into the particles. $v = \frac{c}{n_{eff}}$ is the speed of light in the medium where n_{eff} is the effective refractive index. σ_{em} is the stimulated emission cross section, τ_s is the excited state lifetime, and $D = \frac{vl_t}{3}$ is the light diffusion coefficient where l_t is the transport mean-free-path. We have distinguished between diffusion coefficients for pump and emitted radiation, D_p and D_e, respectively. γ is the fraction of spontaneous emission contributing to the laser process. The reabsorption terms are not included due to the negligible absorption at the emission wavelength (598 nm).

In both cases, the source of diffuse radiation, $p(z,t)$, is an incoming Gaussian pulse in the z direction which is extinguished (scattered and absorbed) along its path through the sample. The expression for the source at OP pumping is written as follows [24]:

$$p_{OP}(z,t) = \frac{J_{OP}}{\exp\left(\frac{z}{l^*}\right)} \frac{\sqrt{\ln 2}}{l_s \Delta \sqrt{\pi}} \exp\left(-\left(\frac{(t - t_{peak} - z/v)}{\Delta} \right)^2 \ln 2 \right). \tag{4}$$

Here, J_{OP} represents the incident photons per unit area at $z = 0$, t_{peak} is the maximum in time of the pump pulse on the sample surface, and Δ is its half width length at half maximum. l_s is the scattering mean-free-path, and l^* is the extinction mean-free-path.

The source of diffuse radiation for TP pumping, $p_{TP}(z,t)$, has been calculated from the solution of the following equation for I (incident photons per unit area and time):

$$\frac{dI}{dz} = -\frac{I}{l_s} - f\beta\, \hbar\, \omega_p I^2 \quad \text{with } I(z=0) = I_{TP} \tag{5}$$

which describes the optical loss of the incoming light through the slab (scattered and absorbed by the TP process). The linear absorption has been neglected. In case of negligible TP absorption ($\beta = 0$), the incoming light would just decay exponentially through the slab due to the scattering processes, as in a single-photon pumping mechanism [24, 28]. After working out Eq. (5), we can write $p_{TP}(z,t)$ as follows:

$$p_{TP}(z,t) = \frac{I_{TP}}{\exp\left(\frac{z}{l_s}\right) - I_{TP}\, \beta\, \hbar\, \omega_p f\, l_s \left(1 - \exp\left(\frac{z}{l_s}\right)\right)} \frac{\sqrt{\ln 2}}{l_s \sqrt{\pi}} \times \exp\left(-\left(\frac{(t - t_{peak} - z/v)}{\Delta} \right)^2 \ln 2 \right). \tag{6}$$

One can estimate the pumping domain depth for both processes by using the diffusive absorption length (l_{abs}) which would be defined for OP and TP process, respectively, as follows:

$$l_{abs}^{OP} = \sqrt{\frac{l_t}{3fK_{abs}}} \text{ and } l_{abs}^{TP} = \sqrt{\frac{l_t}{3f\, \beta\, \hbar\, \omega_p\, W_P(z,t) v}} \tag{7}$$

Notice that the diffusive absorption length defined for TP pumping is dependent on light density at the pump wavelength [16].

The boundary and initial conditions corresponding to a slab geometry in the x–y plane are [24] as follows:

$$\begin{aligned} W_p(-l_e^0, t) = W_p(L + L_e^L, t) = W_e(-l_e^0, t) = W_e(L + L_e^L, t) \quad \forall t \\ W_p(z,0) = W_e(z,0) = N(z,0) = 0 \quad \forall z \end{aligned} \tag{8}$$

where the extrapolation length (l_e) is given by $l_e^{0,L} = \frac{2h_{0,L}}{3} l_t$, with $h_{0,L} = \frac{1+r_{0,L}}{1-r_{0,L}}$. $r_{0,L}$ is the internal reflectivity at the front ($z = 0$) and rear ($z = L$) surfaces, respectively. The time evolution of the reflected flux corresponding to the emitted light is given by $\vec{F}_e = -D_e \frac{\partial W_e}{\partial z} \vec{z}$ evaluated at the sample surface ($z = 0$).

5 Discussion

Theoretical calculations of the variation of the temporal pulse width as a function of the incident pump density have been obtained from the numerical resolution of the three-coupled nonlinear partial differential equations [Eqs. (1)–(3)]. The input values for the calculation are the material parameters: $\sigma_{em} = 2.5 \times 10^{-16}$ cm^2, $K_{abs} = 148.5$ cm^{-1}, τ_s (OP) = 1.65 ns, τ_s (TP) = 2.1 ns, $\beta\hbar\omega_p = 3.86 \times 10^{-13}$ μm ps, $n_{eff} = 1.16$, $f = 0.43$. The mean-free-path lengths at the required wavelengths have been calculated by using the Mie theory for spheres in the independent scatterer approximation with a diameter equal to the averaged mean particle size. These values are displayed in Table 1. The scattering and absorption cross sections and the asymmetry parameters used to obtain these values have been averaged over a size interval $\Delta\phi \sim \lambda$ which is enough for the ripple structure to vanish [29]. The average internal reflectivities of the sample ($r_0 = 0.24$ and $r_L = 0.3$) have been estimated from the Fresnel reflection coefficients by using the effective refractive index of the random system [24, 28], and this refractive index has been calculated from the Maxwell-Garnet theory. The γ parameter ($\gamma = 0.5$) has been estimated from OP pumping measurements [24]. The set of equations, Eqs. (1)–(3), has been numerically solved by the Crank–Nicholson finite difference method, and it has been carried out for a sample with thickness $L = 500$ μm.

Table 1 Characteristic scattering and absorption lengths calculated in the OP and TP regimes

	$\lambda_p = 532$ nm OP absorption	$\lambda_p = 800$ nm TP absorption	$\lambda_{em} = 598$ nm Emission
l_s (μm)	2	2	2
l_t (μm)	8.9	~6.9	9
l_{abs} (μm)	21.6	$\sqrt{\frac{l_t}{3\ \beta\ \hbar\ \omega_p f\ W_P(z,t) v}}$	–

$\beta\ \hbar\ \omega_p = 3.86 \times 10^{-13}$ μm ps and $K_{abs} = 148.5$ cm^{-1} are, respectively, the TP and the OP absorption coefficients. f is the volume fraction occupied by the scatterers ($f = 0.43 \pm 0.05$). Expression for l_{abs} depending on W_p is shown

The theoretically predicted pulse shortening when the excitation density is increased has been plotted in Fig. 2b for each absorption process. As it can be seen, the experimental FWHMs of the output pulse collapses approximately at the same density value than the theoretical FWHMs for both absorption processes. In case of OP excitation, the threshold calculated from the fitting of the theoretical curve to a sigmoid function is 0.52 ± 0.03 mJ/cm^2, whereas the experimental one was 0.54 ± 0.01 mJ/cm^2. In case of TP pumping, the theoretically calculated threshold is 22.5 ± 0.2 mJ/cm^2, whereas the experimental one was 23.3 ± 0.8 mJ/cm^2. In good agreement with the experimental results, the theoretical calculation also demonstrates that the threshold corresponding to TP pumping is higher than the one obtained with single-photon excitation (around 50 times).

The difference between the lasing threshold values of TP and OP regimes could be firstly attributed to the different temporal pumping regimes used, that is, femtosecond regime for TP excitation and picosecond regime for OP excitation. However, the difference in the pumping pulse duration does not explain the observed behavior. We can theoretically predict what happens if both thresholds are compared at the same temporal pump regime. Based on simple models, we can assume that the density of dye molecules in the excited state N for a TP process is proportional to the square of energy density of the pump laser pulse (J_{TP}) and inversely proportional to the pulse duration (Δ), that is, $N \approx I_{TP}^2 \Delta = J_{TP}^2/\Delta$, while for a OP process, it is proportional to J_{OP} and does not depend on the pulse duration. Taking into account these assumptions and provided that the experimental conditions and material characteristics (such as spot size, particle size, volume filling factor) are not changed, we theoretically predict that the TP threshold energy density for a 20-ps laser pulse should be $(200)^{1/2}$ higher than the TP threshold of the 100 fs pulse. Therefore, the different pulse duration of the pump laser is not the reason for the observed deviation between the lasing threshold value at TP and OP processes. However, if we take into account that the pumping domain depth is a crucial parameter closely related to lasing threshold, we could explain the observed behavior by analyzing the way in which the pumping light is absorbed through the sample. In fact, it has already been demonstrated that the lasing threshold in powder lasers decreases as the region where the pumping beam is absorbed diminishes [30].

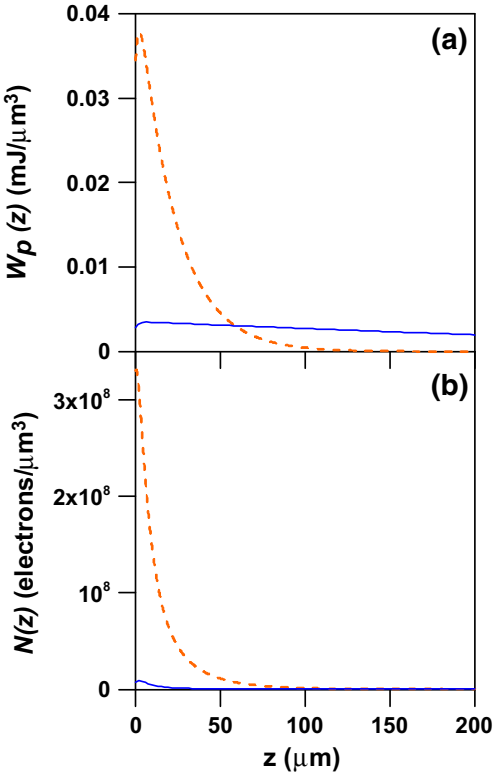

Fig. 3 $W_p(z)$ pump photon density (**a**) and $N(z)$ population inversion (**b**) integrated in time as a function of z for TP (*solid blue line*) and OP (*dashed orange line*) excitations, with identical value of the laser pulse energy density (3.74 mJ/cm^2). The input values for the calculations are the same as in Fig. 2

In Fig. 3, we illustrate the spatial distributions of the light density at the pump wavelength $W_p(z)$ and the excited state population $N(z)$ for both OP and TP processes. These functions would represent the pumping domain depth and the gain region, respectively. They have been calculated by time integration of the $W_p(z,t)$ and $N(z,t)$ functions at identical value of the laser pulse energy density (3.74 mJ/cm^2). The pump energy density chosen is greater than the threshold of the OP process (0.52 mJ/cm^2) and smaller than that corresponding to TP (23.3 mJ/cm^2). As it can be observed, the pumping volume of the random laser for the TP process is larger than that for the OP one (see Fig. 3a) since the light can go much deeper into the material due to the weaker absorption. The light density of the pump beam in the OP process is confined inside a small volume and drops off rapidly due to a limited depth (l_{abs}^{OP}). However, the

density values in the region corresponding to the OP process are much higher than those of the TP one, and consequently, the extraction of the gain can be more effective in the OP process. A similar effect can also be seen in Fig. 3b where the values for the inversion of population corresponding to the OP process through its gain region are much higher than those corresponding to the TP one, and consequently, the system can more easily achieve the critical value to produce laser emission. Therefore, for the same value of the laser pulse energy density, our results obtained for TP excitation indicate that a larger pumping region leads to a lower effective pump density, causing an increase in the lasing threshold.

6 Conclusions

In conclusion, we have experimentally and theoretically demonstrated that a higher TP-pumped lasing threshold is required to achieve random laser action as compared to the usual OP excitation. The sample used has been ground powder of a silica gel containing 2 wt% Rh6G-SiO_2 nanoparticles of 3 μm average particle size. In particular, the random laser threshold in the TP case is around 50 times larger than in OP. The theoretical model based on light diffusive propagation yields a good agreement with the experimental results corresponding to the TP excitation as well as a fairly good prediction for the ratio between two and OP-pumped random laser thresholds. We expect this work will promote extended studies of RL in stronger TP absorbing media which can be functionalized and therefore potentially used as biomedical sensors or biotracers.

Acknowledgments This work was supported by the Spanish Government MEC (FIS2011-27968 and TEC 2012-37983-C03-01), Basque Country Government (IT-659-13 and IT-664-13), and by the University of the Basque Country (UPV/EHU) through program UFI 11/16. S. G.-R acknowledges the financial support from Research Association MPC for a postdoctoral appointment. The authors are grateful to Dr. M. Al-Saleh for sample preparation and would also like to thank SGIker ARINA from the University of the Basque Country (UPV/EHU) for allocation of computational resources.

References

1. G.S. He, C. Lu, Q. Zheng, A. Baev, M. Samoc, P.N. Prasad, Phys. Rev. A **73**, 033815 (2006)
2. G.S. He, T.-G. Lin, S.-J. Chung, Q. Zheng, C. Lu, Y. Cui, P.N. Prasad, J. Opt. Soc. Am. B **22**, 2219 (2005)
3. H. Cao, Waves Random Media **13**, R1 (2003)
4. M.A. Noginov, *Solid-State Random Lasers* (Springer, Berlin, 2005)
5. D.S. Wiersma, Nat. Phys. **4**, 359 (2008)
6. D.S. Wiersma, A. Lagendijk, Phys. Rev. E **54**, 4256 (1996)
7. X. Jiang, C.M. Soukoulis, Phys. Rev. Lett. **85**, 70 (2000)
8. A.L. Burin, M.A. Ratner, H. Cao, R.P.H. Chang, Phys. Rev. Lett. **87**, 215503 (2001)
9. S. Mujumdar, V. Turck, R. Torre, D.S. Wiersma, Phys. Rev. A **76**, 033807 (2007)
10. H.E. Türeci, Science **320**, 643 (2008)
11. O. Zaitsev, L. Deych, J. Opt. **12**, 024001 (2010)
12. J. Andreasen, A.A. Asastryan, L.C. Botten, M.A. Byrne, H. Cao, L. Ge, L. Labonté, P. Sebbah, A.D. Stone, H.E. Türeci, C. Vanneste, Adv. Opt. Photon. **3**, 88 (2011)
13. J. Andreasen, N. Bachelard, S.B.N. Bhaktha, H. Cao, P. Sebbah, C. Vanneste, Int. J. Mod. Phys. B **28**, 1430001 (2014)
14. M. Leonetti, C. Conti, C. López, Phys. Rev. A **88**, 043834 (2013)
15. G. Zacharakis, N.A. Papadogiannis, T.G. Papazoglou, Appl. Phys. Lett. **81**, 2511 (2002)
16. A.L. Burin, H. Cao, M.A. Ratner, IEEE J. Sel. Top. Quantum Electron. **9**, 124 (2003)
17. K. Wang, J. Liu, J. Lu, D. Xu, Opt. Quantum Electron. **37**, 1001 (2005)
18. R.C. Polson, Z.V. Vardeny, Appl. Phys. Lett. **85**, 1289 (2004)
19. J. Chen, H. Mizuno, H. Kawano, A. Miyawaki, K. Midorikawa, Appl. Phys. B **85**, 45 (2006)
20. G. Zhu, C.E. Small, M.A. Noginov, Opt. Lett. **33**, 920 (2008)
21. E.V. Chelnokov, N. Bityurin, I. Ozerov, W. Marine, Appl. Phys. Lett. **89**, 17119 (2006)
22. S. García-Revilla, I. Sola, R. Balda, L. Roso, D. Levy, M. Zayat, J. Fernández, Proc. SPIE **7598**, 759804 (2010)
23. N.S. Makarov, M. Drobizhev, A. Rebane, Opt. Express **16**, 4029 (2008)
24. S. García-Revilla, J. Fernández, M.A. Illarramendi, B. García-Ramiro, R. Balda, H. Cui, M. Zayat, D. Levy, Opt. Express **16**, 12251 (2008)
25. W.L. Sha, C.H. Liu, R.R. Alfano, Opt. Lett. **19**, 1922 (1994)
26. M. Siddique, R.R. Alfano, G.A. Berger, M. Kempe, A.Z. Genack, Opt. Lett. **21**, 450 (1996)
27. G. Zacharakis, G. Heliotis, G. Filippidis, D. Anglos, T.G. Papazoglou, Appl. Opt. **38**, 6087 (1999)
28. B. García-Ramiro, M.A. Illarramendi, I. Aramburu, J. Fernández, R. Balda, M. Al-Saleh, J. Phys.: Condens. Matter **19**, 456213 (2007)
29. C.F. Bohren, D.R. Huffman, *Absorption and Scattering of Light by Small Particles* (Wiley, New York, 1983)
30. B. García-Ramiro, I. Aramburu, M.A. Illarramendi, J. Fernández, R. Balda, Eur. Phys. J. D **52**, 195 (2009)